



Waves in Excitable Media

Author(s): J. P. Keener

Source: *SIAM Journal on Applied Mathematics*, Vol. 39, No. 3 (Dec., 1980), pp. 528-548

Published by: Society for Industrial and Applied Mathematics

Stable URL: <http://www.jstor.org/stable/2100722>

Accessed: 07-06-2018 15:22 UTC

JSTOR is a not-for-profit service that helps scholars, researchers, and students discover, use, and build upon a wide range of content in a trusted digital archive. We use information technology and tools to increase productivity and facilitate new forms of scholarship. For more information about JSTOR, please contact support@jstor.org.

Your use of the JSTOR archive indicates your acceptance of the Terms & Conditions of Use, available at <http://about.jstor.org/terms>



Society for Industrial and Applied Mathematics is collaborating with JSTOR to digitize, preserve and extend access to *SIAM Journal on Applied Mathematics*

WAVES IN EXCITABLE MEDIA*

J. P. KEENER†

Abstract. A general class of two-component reaction-diffusion systems with excitable dynamics is studied by means of singular perturbation theory. It is shown how stable traveling pulses and periodic wavetrains in one spatial dimension evolve from initial data. This information is applied to two-dimensional regions for which it is shown that steady rotating structures (spirals) exist.

The perturbation results are also used to show that a one-dimensional semi-infinite medium exhibits hysteresis when used as a periodic signaling device. Finally, other nonexcitable dynamics are analyzed, and their stable one-dimensional structures listed.

Introduction. In this paper we address three general questions. First, what is the structure of waves which propagate in an excitable medium and how do they evolve from initial data? Second, how do waves propagate in a two-dimensional excitable medium? Finally, what types of self-sustaining structures can be seen in a two-dimensional medium, and how do they evolve from initial data?

There are at least two physiological contexts in which questions of this nature arise. In nerve fibers, pulses of electrical activity may travel without attenuation provided the pulses are initiated properly and at the right time, while other pulses may fail to propagate. In muscle tissues, such as heart muscle, similar phenomena are observed, but the fact that these media are not one-dimensional is an important consideration. For example, atrial flutter and fibrillation can occur in these higher dimensional excitable media ([26]). In chemical reactions, such as the Belousov-Zhabotinsky reaction, two-dimensional patterns such as spirals and expanding target patterns have been observed ([27], [28]), but not adequately analyzed.

Traveling pulses and periodic wavetrains have been found for specific one-dimensional excitable media models by a number of investigators ([3], [4], [14], [24]), although the evolution from initial data onto these solutions was not discussed. Other investigators have used singular perturbation methods to analyse traveling fronts in media with self-oscillatory dynamics or multiple steady states ([8], [22]), and with a caricature of the Fitzhugh-Nagumo dynamics ([25]).

Much of the analytical work on spatial structure in two-dimensional media has relied on self-oscillatory dynamics. For example, slowly varying plane waves ([16], [18]), spirals, and pacemakers ([16], [5]) have been found assuming oscillatory dynamics at the start.

In [26] it was assumed that wavefronts in an excitable medium move normal to themselves with constant velocity. With this simple assumption, it is easy to demonstrate that spiral waves exist in multiply connected domains. Spirals have also been calculated numerically using simple piecewise linear excitable dynamics ([29]), and using a discrete caricature of an excitable medium ([7], [13], [19], [21]). In this latter case, the medium is divided into a finite number of cells and the state of the medium in the cells is characterized by one of a finite number of integers. Rules are devised on how diffusion affects neighboring cells in different states as time passes. Patterns which evolve from specified initial data are then easily calculated with a digital computer. (See also the "Game of Life" [11].)

* Received by the editors June 26, 1979. This research was supported in part by the National Science Foundation under Grant MCS 75-07621.

† Department of Mathematics, University of Utah, Salt Lake City, Utah 84112.

Experiments in excitable media suggest that spiral waves can occur. One such set of experiments ([25]) was performed on the cortex of a rat in which an interior region was anesthetized. Very precise stimulation patterns were necessary to initiate a spiral wave (called reverberating cortical spreading depression) which then continued indefinitely. It is suggested ([26], [21]), that atrial flutter is also the result of spiral activity. However, initial data to initiate such a state are again difficult to attain.

In addition to spirals, other wave patterns such as expanding target patterns have been observed in chemical reactions ([28]). One interesting observation about these target patterns is that different centers can produce rings at different frequencies and that the higher frequency pacemakers eventually annihilate those of lower frequency.

This paper is divided into two parts. The first part (§§ 1.1–1.4) deals with the existence and structure of waves in a one-dimensional excitable medium and examines the response of the medium to various initial data. The techniques used are singular perturbation methods in terms of a small parameter ε which is the ratio of the rates of growth of the two state variables of the medium. In addition to the basic analysis of the initial value problem, we demonstrate in § 1.5 that if the medium is used as a signaling device, stimulated at a local site with period T , then the “downstream” response to the periodic input exhibits a curious hysteresis. The results of our perturbation analysis are confirmed by some numerical computations performed by J. Rinzel which we present in § 1.6. Finally, we use the ideas and results of this analysis to discuss briefly other types of nonexcitable dynamics. Included in these are dynamics of relaxation oscillation type for which the dispersion relation for periodic wave propagation is calculated.

The second part of this paper deals with two-dimensional wave patterns. Extending the singular perturbation analysis of Part I, we are able to demonstrate the existence of rotating spirals in a multiply connected region, as well as other phenomena such as the interaction of target patterns of different frequency mentioned above.

For the general excitable dynamics assumed here, explicit calculations needed for this analysis are extremely difficult. However, all of the calculations can be carried out for the simple piecewise linear dynamics used by other investigators as an approximation to the Fitzhugh-Nagumo equations.

PART I. The formation and evolution of waves in an excitable medium.

1.1. Background. Throughout this paper we consider the system of diffusion reaction equations

$$(1.1) \quad \begin{aligned} \varepsilon u_t &= \varepsilon^2 D_1 \nabla^2 u + f(u, v), \\ v_t &= \varepsilon^2 D_2 \nabla^2 v + g(u, v), \end{aligned}$$

where $\varepsilon \ll 1$, ∇^2 is the Laplacian in one or two spatial dimensions, and the general shapes of the functions f and g are as indicated in Fig. 1. In particular we assume that the neutral curve $f(u, v) = 0$ is cubic in shape, in that there are three distinct functions $u = u_-(v)$, $u = u_*(v)$ and $u = u_+(v)$ for which $f(u(v), v) = 0$. These three curves are defined on the regions $v \geq v_{\min}$, $v_{\min} \leq v \leq v_{\max}$, and $v \leq v_{\max}$, respectively. The function $f(u, v)$ is negative above and positive below the curve $f(u, v) = 0$.

The function $g(u, v)$ is assumed to be negative above (to the left) and positive below (to the right) of the neutral curve $g(u, v) = 0$. The curve $g(u, v) = 0$ has one intersection with the curve $f(u, v) = 0$ located on the curve $u = u_-(v)$. This intersection, denoted by (u_0, v_0) , is the unique, steady, stable, uniform solution of (1.1).

The general structures of f and g are typical of excitable dynamics. A vague definition of excitability is that a small deviation of the state variables from the unique stable steady state (u_0, v_0) leads to a large excursion from the steady state before the

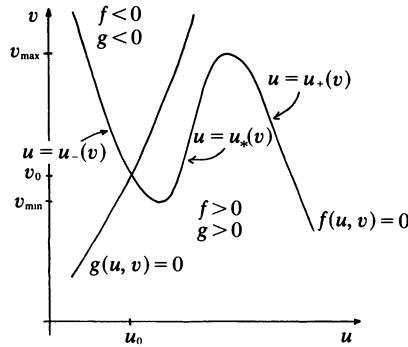


FIG. 1

eventual return to it ([29]). A more satisfactory definition ([17]) is that with a sufficient initial stimulus, a pulse can be initiated which propagates throughout the medium.

The dynamics we have assumed here are certainly excitable in the first sense. In fact, any initial values of u, v for which $v < v_{\min}$ or for which $u > u_+(v)$ are said to be superthreshold, since the resulting dynamics do not return directly to the steady state (u_0, v_0) . We shall see, however, that the existence of a threshold is not sufficient to guarantee that a pulse can propagate throughout the medium. In fact, although a pulse may be initiated, it may slow down, reverse direction, and eventually annihilate itself, thus failing to propagate throughout the medium.

The cubic structure of the function f is typical of many chemical reactions involving activation and inhibition ([2]). The best known example is the Fitzhugh–Nagumo model for chemical–electrical conduction in a nerve ([15], [20]), for which

$$\begin{aligned} f(u, v) &= -u(u - \alpha)(u - 1) - v, & 0 < \alpha < 1, \\ g(u, v) &= u - dv, \\ D_2 &= 0, & D_1 = 1, \end{aligned} \quad (1.2)$$

Many of the questions we address in this paper are suggested by questions of propagation of pulses in nerve fiber which are modeled by these equations.

Even in the specific form of (1.2), there are difficulties which make explicit computation impossible. For this reason the piecewise linear approximation

$$\begin{aligned} f(u, v) &= -u - v + H(u - \alpha), \\ g(u, v) &= u, \\ D_2 &= 0, & D_1 = 1, \end{aligned} \quad (1.2)'$$

has been used to calculate explicitly many of the properties of traveling pulses and periodic waves of (1.1), ([20], [24]). The perturbation analysis we give for (1.1) can be carried out explicitly for (1.2)'. For purposes of illustration, we will make reference to this model throughout our discussion.

The structure of g is also critical to the excitable nature of the medium. Moderate changes in g lead to self-oscillatory dynamics, multiple steady states, etc. The analysis we present here applies to these other situations which we will discuss in a later section. However, our primary emphasis is on the case of excitable dynamics.

1.2. The formation of pulses. Suppose that we have a one-dimensional excitable medium governed by (1.1) with $\nabla^2 \equiv \partial^2 / \partial x^2$, and suppose that initial data $u_0(x), v_0(x)$

are prescribed for (1.1) on the entire real line $-\infty < x < \infty$. Typically $u_0(x)$ and $v_0(x)$ approach (u_0, v_0) as $x \rightarrow \pm\infty$. Since $\varepsilon \ll 1$, there will be an initial layer on the fast time scale $\tau = t/\varepsilon$. During this $O(\varepsilon)$ time period the solution will be governed, to first order in ε , by the equations

$$(1.3) \quad u_\tau = f(u, v), \quad v_\tau = 0.$$

From (1.3) we learn that u rapidly equilibrates to a stable solution of $f(u, v) = 0$ while v remains fixed. For many values of x , this equilibration will be to $u = u_-(v)$. However if the initial values for u are superthreshold, the equilibrium will be $u = u_+(v)$. Near any point with initial data exactly on the threshold curve, the dynamics (1.3) cause a rapid spatial change in the variable u . Because of diffusion in (1.1), this rapid change in u destroys the validity of (1.3), and near any such point a different scaling of the variables is needed.

If at $x = x_0$ the initial data are on the threshold curve, i.e., $u_0(x) = u_*(v_0(x))$ for $x = x_0$, we can examine the initial equations near $x = x_0$ by introducing a second scaled variable $\xi = (x - x_0)/\varepsilon$. To first order in ε , (1.1) becomes

$$(1.4) \quad \begin{aligned} u_\tau &= D_1 u_{\xi\xi} + f(u, v), \\ v_\tau &= 0. \end{aligned}$$

Since $v_\tau = 0$ we have that

$$(1.5) \quad \begin{aligned} v &= v_0(x) = v_0(\varepsilon\xi), \\ u_\tau &= D_1 u_{\xi\xi} + f(u, v_0(\varepsilon\xi)), \\ u(\xi, \tau)|_{\tau=0} &= u_0(\varepsilon\xi) = u_0(x). \end{aligned}$$

Equations similar to (1.5) have been studied in the context of propagation of genetic traits ([1], [9], [10]). Although many things are known about equations of the form (1.5), the important fact we need is that with initial data specified, a wave front is set up providing a smooth transition between the two stable zeros of $f(u, v(x_0))$, namely $u_-(v(x_0))$ and $u_+(v(x_0))$. The fact that this front also moves with a certain velocity will be discussed and exploited in later sections.

In summary, initial data which lie on the threshold curve produce shocks of thickness $O(\varepsilon)$ which are transitions between the curves $u_-(v)$ and $u_+(v)$ for the threshold value of v . Since this takes place on a time interval $O(\varepsilon)$, the front which is formed can move at most a distance which is also $O(\varepsilon)$ from its initial location in space during this initial time interval.

1.3. The leading edge. After the initial time period has passed, the phase portrait of u and v lies on the neutral curve $f(u, v) = 0$ everywhere except at those points where sharp fronts have been formed for fixed values of v . As time evolves, we expect two things to happen to the shocks. First, the shocks will move in space with some velocity to be determined, and second, the value of v internal to the shock will change.

Suppose that at time t there is a shock at location $x = y(t)$. To examine the dynamics of this shock we make the change of variables

$$(1.6) \quad \xi = x - y(t), \quad \tau = t.$$

With this change of variables the equations (1.1) become

$$(1.7) \quad \begin{aligned} \varepsilon(u_\tau - y'(\tau)u_\xi) &= \varepsilon^2 D_1 u_{\xi\xi} + f(u, v), \\ v_\tau - y'(\tau)v_\xi &= g(u, v) + \varepsilon^2 D_2 v_{\xi\xi}. \end{aligned}$$

To lowest order in ε , these equations reduce to

$$(1.8) \quad v_\tau - y'(\tau)v_\xi = g(u, v), \quad f(u, v) = 0.$$

Since $f(u, v) = 0$, we must have $u = u_\pm(v)$, in which case

$$(1.9) \quad v_\tau - y'(\tau)v_\xi = G_\pm(v) \equiv g(u_\pm(v), v).$$

Equation (1.9) is valid away from the shock, and is called the outer solution.

Equation (1.9) is a first-order hyperbolic equation which can be written in the form

$$(1.10) \quad \frac{dv}{d\tau} = G_\pm(v) \quad \text{on} \quad \frac{d\xi}{d\tau} = y'(\tau).$$

In this form, (1.10) can be readily solved with given initial data provided $y'(\tau)$ is known. Assume for the moment that $y'(\tau)$ is known. Then $v(\tau)$ evolves along a characteristic according to (1.10) until the characteristic reaches the fixed shock position $\xi = 0$. As the characteristic moves through the shock position $\xi = 0$, the derivative of v undergoes a discontinuous change from $G_+(v)$ to $G_-(v)$ or vice versa, while v remains continuous across the shock. We define the front of the shock as that region in which characteristics move toward the shock. Then we observe that the value of v internal to the shock is determined by the dynamics of v ahead of the shock. This fact was implied in [8], and derived explicitly in [23] for (1.2)'.

In terms of the original variables, the outer solution has the form

$$(1.11) \quad \frac{dv}{dt} = G_\pm(v), \quad f(u, v) = 0.$$

This description merely tells us that away from a shock the state variables evolve according to their phase plane dynamics. What this description does not state is how the dynamics away from a shock influence the value of v inside the shock.

To determine $y'(\tau)$, the speed of the shock, we must examine the structure of the shock in more detail. To do so we change the scale of the spatial variable ξ by making the change of variables $\eta = \xi/\varepsilon$. With this change of variables, (1.7) becomes

$$(1.12) \quad D_1 u_{\eta\eta} + y'(\tau)u_\eta + f(u, v) = \varepsilon u_\tau,$$

$$(1.13) \quad y'(\tau)v_\eta = \varepsilon(v_\tau - g(u, v) - D_2 v_{\eta\eta}).$$

To first order in ε , these inner equations reduce to

$$(1.14) \quad D_1 u_{\eta\eta} + y'(\tau)u_\eta + f(u, v) = 0, \quad v_\eta = 0.$$

Clearly, v must be independent of η inside the shock. Furthermore, in order to match this inner solution with the outer solution we must have

$$(1.15) \quad f(u, v) = 0 \quad \text{as} \quad \eta \rightarrow \pm\infty.$$

The important observation about (1.13) is that since $y'(\tau)$ and v depend only on τ , we have an ordinary differential equation in η parameterized by τ . Furthermore, for each fixed v there is a unique eigenvalue $c = c_\pm(v)$ for which

$$(1.16) \quad D_1 u'' + c_\pm u' + f(u, v) = 0, \quad \begin{cases} u \rightarrow u_+(v) & \text{as } \eta \rightarrow \pm\infty, \\ u \rightarrow u_-(v) & \text{as } \eta \rightarrow \mp\infty. \end{cases}$$

Notice that $c_-(v) = -c_+(v)$. The sign of c_+ is easily determined by multiplying (1.16) by

u' and integrating from $\eta = -\infty$ to $\eta = +\infty$. Doing so we find that

$$(1.17) \quad c_+ = \frac{-\int_{u_-(v)}^{u_+(v)} f(u, v) du}{\int_{-\infty}^{\infty} u'^2(\eta) d\eta},$$

so that c_+ has the opposite sign from $\int_{u_-}^{u_+} f(u, v) du$. Thus, if a shock has internal structure determined by v , it must travel with speed $y'(\tau) = c_{\pm}(v(\tau))$.

According to our assumptions on $f(u, v)$, the speed $c_+(v)$ defined by (1.16) is negative for small $v > v_{\min}$ and positive for large $v < v_{\max}$. For simplicity, we assume that $c_+(v)$ is a monotonic increasing function of v with a unique zero. For the Fitzhugh-Nagumo caricature (1.2)', c_+ can be calculated directly and is

$$(1.18) \quad c_+(v) = \frac{2(\alpha + v - 1/2)}{\sqrt{(\alpha + v)(1 - \alpha - v)}}.$$

With this information, we are able to understand the formation and propagation of a leading shock. After the initial evolution described in the previous section, v is essentially unchanged from its initial values, while u lies on one of the neutral curves $u = u_{\pm}(v)$. Suppose that a shock is formed with value v at position $x = y(0)$. Then $u = u_-(v)$ on one side and $u = u_+(v)$ on the other side of $x = y(0)$. For the value of v internal to the newly formed shock, the speed $c = c_{\pm}(v)$ is determined by the eigenvalue problem (1.16) with the orientation of the boundary data at $\eta = \pm\infty$ chosen to match the orientation of the outer solution. The sign of c determines the front and back of the shock; if $c > 0$ the region ahead of the shock is $x > y(t)$, and so forth. As the shock moves, the value of v inside the shock changes according to the outer dynamics of v ahead of the shock, which in turn determines the speed with which the shock continues to move.

One can use (1.10) and (1.14) to find the position and internal value v of the leading shock. For definiteness we suppose that $u = u_-(v)$ for $x < y(0)$ and $u = u_+(v)$ for $x > y(0)$. Suppose the value of v at $x = y(0)$ has $c_+(v) < 0$ and that initial data $v_0(x) \rightarrow v_0$ as $x \rightarrow -\infty$. Then at position $x < y(0)$ after time t the value of v is given implicitly by

$$(1.19) \quad \int_{v_0(x)}^v \frac{dv}{G_-(v)} = t.$$

If the value v determined by (1.19) is also the value of v internal to the shock, then the position of the shock is determined by

$$(1.20) \quad \frac{ds}{dt} = c_+(v), \quad s(0) = y(0).$$

Using (1.19) to define $v = v(t, v_0(x))$, we observe that (1.20) reduces to

$$(1.21) \quad \frac{ds}{dt} = c_+(v(t, v_0(s))), \quad s(0) = y(0).$$

The first order nonlinear differential equation (1.21) for s has some interesting and important properties. First, notice that $v(t, v_0(s)) \rightarrow v_0$ as $t \rightarrow \infty$ or as $s \rightarrow -\infty$. Therefore, if $c_+(v_0) < 0$, the asymptotic speed of the shock will be

$$(1.22) \quad \frac{ds}{dt} = c_+(v_0),$$

and the value of v internal to the shock will eventually be $v = v_0$.

PROPOSITION 1. Suppose that v^* is the unique value of v for which

$$(1.23) \quad \int_{u_-(v^*)}^{u_+(v^*)} f(u, v^*) du = 0.$$

Then if $v_0 < v^*$ the medium is excitable; there are stable pulses which propagate throughout the medium.

PROPOSITION 2. Suppose that a shock is formed for some value $v < v^*$, and that ahead of the shock the initial data also satisfy $v_0(x) < v^*$. Then the shock which forms will propagate through the medium with asymptotic speed $|c_+(v_0)|$.

There are a number of ways that a shock can form but fail to propagate throughout the medium. First, if two shocks moving in opposite directions meet they annihilate each other. Second, if $v > v^*$ then the sign of $c(v)$ is reversed and ahead of the shock the initial data are on $u = u_+(v)$. This shock must collapse and disappear, since the dynamics on $u = u_+(v)$ are valid for only a finite amount of time.

If $c_+(v_0) > 0$, even though the shock forms for $v < v_0$ with $c_+(v) < 0$, the value of v internal to the shock will reach v^* in a finite amount of time after which time the direction of propagation of the shock is reversed, and $u = u_+(v)$ ahead of the shock. According to the previous paragraph, this shock must eventually collapse. Thus, we see that if $c_+(v_0) > 0$ the medium is not excitable. For the remainder of this paper we assume that the medium is excitable; i.e., $v_0 < v^*$.

For the Fitzhugh-Nagumo models (1.2) and (1.2)', we easily calculate that

$$(1.24) \quad v^* = \frac{2}{27}(\alpha - 1/2)(\alpha - 2)(\alpha + 1),$$

and

$$(1.24)' \quad v^* = \frac{1}{2} - \alpha,$$

respectively. In both cases $v_0 = 0$, so that we have an excitable medium whenever $\alpha < \frac{1}{2}$, which is a well-known result.

1.4. The trailing shock. The role of the leading shock is to excite the medium. As it moves, the leading shock provides a sharp transition between $u = u_-(v)$ ahead and $u = u_+(v)$ behind. At any point in space, the state variables can remain in the excited state $u = u_+(v)$ for at most a finite amount of time, since the outer solution does not make sense for $v > v_{\max}$. As a result, somewhere behind the leading shock there must be a trailing shock to provide a sharp transition between $u = u_+(v)$ ahead and $u = u_-(v)$ behind. Notice that a trailing shock cannot exist indefinitely on its own, but requires that there be a leading shock continually exciting the medium ahead of the trailing shock.

The behavior of the trailing shock is again described by the inner and outer equations (1.11) and (1.14), where the medium ahead of the shock is excited to $u = u_+(v)$ by a leading shock and behind is in the resting state $u = u_-(v)$. If the trailing shock occurs for a value v , then the speed with which this shock must travel is $c_{\pm}(v)$, determined by (1.16) where the sign chosen is opposite the appropriate sign for the leading shock. This opposite choice of sign guarantees that a leading shock with $v < v^*$ and a trailing shock with $v > v^*$ travel in the same direction.

Now suppose that the internal structure $v_1 = v_1(t)$ and speed $c = c_{\pm}(v_1)$ of the leading shock are known. Then a trailing shock with internal structure $v_2 = v_2(t)$ is initiated at some point. Unless the initial data produce a shock with $v > v^*$, this shock will be initiated at $v_2 = v_{\max}$ by the outer solution (1.10). After this initiation the

separation s_1 between these two shocks satisfies

$$(1.25a) \quad \frac{ds_1}{dt} = c_{\pm}(v_1(t)) - c_{\mp}(v_2).$$

The separation between the two shocks must also satisfy

$$(1.25b) \quad s_1 = \int_{t-\tau}^t c_{\pm}(v_1(\eta)) d\eta,$$

where

$$(1.25c) \quad \tau = \int_{v_1(t-\tau)}^{v_2} \frac{dv}{G_{+}(v)}.$$

Equation (1.25b) determines $\tau = \tau(s_1)$ implicitly, and (1.25c) determines $v_2 = v_2(\tau, v_1(t-\tau))$. These two equations together provide $v_2 = v_2(s_1, v_1(t-\tau(s_1)))$, which imply that

$$(1.26) \quad \frac{ds_1}{dt} = c_{\pm}(v_1(t)) - c_{\mp}(v_2(s_1, v_1(t-\tau(s_1)))).$$

The first order nonautonomous equations (1.26) determines the separation s_1 between the leading and trailing shocks, and this separation in turn determines the value v_2 through (1.25b,c).

The main observation we make about (1.26) is that since $v_1(t)$ is determined from initial data by (1.21), and since for large t , $v_1(t) \rightarrow v_0$, $c_{\pm}(v_1) \rightarrow c_{\mp}(v_0)$, (1.26) becomes (essentially) autonomous for large time. As $t \rightarrow \infty$, (1.26) becomes

$$(1.27a) \quad \frac{ds_1}{dt} = c_{\pm}(v_0) - c_{\mp}(v_2(s_1, v_0)),$$

where v_2 is determined from

$$(1.27b) \quad s_1 = c_{\pm}(v_0) \int_{v_0}^{v_2} \frac{dv}{G_{+}(v)}.$$

Since $c_{\pm}(v)$ is (by assumption) a monotonic function of v , (1.27), and hence (1.25), has a unique asymptotic solution, with v_2 approaching the unique value v for which $c_{\mp}(v_2) = c_{\pm}(v_0)$ and with spatial separation between the two shocks approaching the value determined by (1.27b).

This analysis fails if $|c_{\pm}(v_{\max})| < |c_{\mp}(v_0)|$, so that the trailing shock occurs at $v = v_{\max}$. Appropriate modifications to the inner solution at the trailing shock must be made in this case. Here we assume that this is not a problem. In fact, for the Fitzhugh-Nagumo equation (1.2) and (1.2)', $c_{+}(v) = c_{-}(2v^{*} - v)$, so that there is always a steady solution for (1.25), with $v_2 = 2v^{*}$ since $v_0 = 0$.

We have now seen how a stable pulse emerges from specified initial data. The asymptotic shape of this pulse is precisely that found by a singular perturbation analysis in [4]. However this solitary pulse is not the only structure that can be produced by initial data. We discuss some of these other possibilities in the next section.

1.5. Periodic wavetrains and signaling. Exploring further the ideas of § 1.4, one can easily construct sequences of pulses. In order that all the pulses travel in the same direction, the sequence of pulses must alternate between leading ($v < v^{*}$) and trailing ($v > v^{*}$) pulses. We can calculate the separation s_k between the k th and $k + 1$ st shock by induction.

Suppose the k th shock has internal structure $v_k(t)$. Then

$$(1.28a) \quad \frac{ds_k}{dt} = c_{\pm}(v_k(t)) - c_{\mp}(v_{k+1}(t)),$$

where

$$(1.28b) \quad s_k = \int_{t-\tau_k}^t c_{\pm}(v_k(\eta)) d\eta,$$

$$(1.28c) \quad \tau_k = \int_{v_k(t-\tau_k)}^{v_{k+1}} \frac{dv}{G_{\pm}(v)},$$

and where the signs in (1.28a,b) are chosen by the appropriate boundary condition in (1.16). The $+$ sign is chosen in (1.28c) if v_k is a leading shock. As before, (1.28) can be re-expressed as

$$(1.29) \quad \frac{ds_k}{dt} = c_{\pm}(v_k(t)) - c_{\mp}(v_{k+1}(s_k, v_k(t - \tau_k(s_k)))).$$

Equation (1.29) can be used to understand the structure of an infinite sequence of pulses. In particular, to have periodic pulses we must have $c_{\pm}(v_k) = c_{\mp}(v_{k+1})$. Furthermore, the period T and wavelength Λ of these periodic wavetrains are

$$(1.30) \quad T = \int_{v_k}^{v_{k+1}} \frac{dv}{G_{+}(v_k)} + \int_{v_{k+1}}^{v_k} \frac{dv}{G_{-}(v)},$$

$$\Lambda = |c_{\pm}(v_k)|T,$$

respectively, where v_k is assumed to be a leading shock and v_{k+1} satisfies $c_{\pm}(v_k) = c_{\mp}(v_{k+1})$.

If v_k can somehow be constrained so that v_k is a constant $v_k \neq v_0$, then the shocks that follow v_k are asymptotically attracted to the steady periodic wave train with speed $|c_{+}(v_k)|$. In this way, the periodic wavetrains are stable to spatial perturbations.

Finally, notice that since $G_{-}(v_0) = 0$, then $T \rightarrow \infty$ if $v_k \rightarrow v_0$. In other words, the leading shocks in a periodic wavetrain must have $v_k > v_0$ and the speed of the periodic wavetrain is smaller than the speed of the solitary pulse. Unfortunately, the validity of (1.30) breaks down as $v_k \rightarrow v^*$ and $c(v_k) \rightarrow 0$.

The second problem we discuss in this section is that of signaling on a semi-infinite one-dimensional medium. Suppose we stimulate the medium at a fixed site with period T , and observe how many of the stimulations (firings) result in a pulse which propagates throughout the medium.

At each firing we give a large positive impulse to the variable u while keeping v fixed. In the language of Fitzhugh-Nagumo variables, this means that at regular time intervals of length T we give a fixed large stimulus to the voltage. The size of the input is always large enough so that for any value of v with $u = u_{-}(v)$, the input is super-threshold. Our analysis will be carried out in the singular limit $\varepsilon \rightarrow 0$.

The response of the medium to one of these impulses is easy to describe. At the time of the impulse the medium at the impulse site experiences a rapid excursion from $u_{-}(v)$ to $u_{+}(v)$ with v fixed. A front is initiated and begins to move away from the impulse site with speed $|c_{\pm}(v)|$. If $v < v^*$ and if $u = u_{-}(v)$ at the time of the impulse, the resulting front will propagate throughout the medium at a rate of speed determined by (1.28). If $v > v^*$, the pulse fails to propagate into the medium, and if u is already in the excited state $u = u_{+}(v)$ at the time of firing, the impulse has no effect on the medium.

If a front does result from a firing, then at a later time governed by the outer solution, the medium at the impulse site will experience a rapid excursion at $v = v_{\max}$ from $u_+(v_{\max})$ to $u_-(v_{\max})$, and thereby initiate a trailing front which must propagate through the medium behind the leading shock as described by (1.25). After the trailing shock is initiated, the medium relaxes toward (u_0, v_0) along with $u = u_-(v)$ with $v_t = G_-(v)$. A subsequent impulse repeats this process.

To analyze this process we must keep track of the value of v at each firing, since this value characterizes the response of the medium. We do this by means of a mapping

$$(1.31) \quad v_{k+1} = M_T(v_k),$$

where v_k is the value of v for the k th successful firing, and where T is the period of the impulse. There is no need to keep track of unsuccessful firings since the medium is unaffected by these.

We define the mapping (1.31) entirely in terms of the outer solution, and ignore the $O(\varepsilon)$ transition times of the leading and trailing shocks. Define the number T^* to be the "return time" of a pulse formed with $v = v^*$,

$$(1.32) \quad T^* = \int_{v^*}^{v_{\max}} \frac{dv}{G_+(v)} + \int_{v_{\max}}^{v^*} \frac{dv}{G_-(v)} \equiv \int_{v^*}^{v_{\max}} \left[\frac{1}{G_+(v)} - \frac{1}{G_-(v)} \right] dv.$$

Then the mapping (1.31) is defined implicitly as the largest value of $v < v^*$ for which

$$(1.33) \quad pT = \int_{v_k}^{v_{\max}} \frac{dv}{G_+(v)} + \int_{v_{\max}}^v \frac{dv}{G_-(v)},$$

with p an integer. If n is the smallest integer for which $nT \geq T^*$, then $p \geq n$. Notice that $p - 1$ is the number of firings which were ignored by the medium between successful firings. In what follows, we assume that the firing mapping M_T is a local contraction; i.e., for two values $v_i < v^*$, $i = 1, 2$, the resulting values of v under M_T after time nT , say \hat{v}_i , satisfy

$$(1.34a) \quad |\hat{v}_1 - \hat{v}_2| < |v_1 - v_2|,$$

where

$$(1.34b) \quad nT = \int_{v_i}^{v_{\max}} \frac{dv}{G_+(v)} + \int_{v_{\max}}^{v_i} \frac{dv}{G_-(v)}, \quad i = 1, 2.$$

We can summarize the properties of the mapping (1.31) as follows:

PROPOSITION 3. *The mapping (1.31) is a piecewise continuous mapping of the interval $[v_0, v^*]$ into itself with at most one jump discontinuity. For every value of v except the discontinuity, the function M_T has a derivative which satisfies $-1 < M'_T < 0$. For each fixed value of T , there are either one or two stable fixed points of the mapping (1.29) which depend continuously on T . For each integer n there is an interval (t_n, s_n) such that for $T \in (t_n, s_n)$ there is an attracting fixed point of (1.33) for $p = n$. Furthermore, $t_n < s_{n+1}$, so that successive intervals overlap.*

The main consequence of this statement is that for each value of T in the interval (t_n, s_n) , the medium responds to the T -periodic input with nT periodic response. Since the intervals overlap there is an observed hysteresis if the parameter T is changed slowly.

To demonstrate these facts, we suppose that $nT > T^* > (n-1)T$. Then $M_T(v^*) < v^*$ and the preimage of v^* , say $v^{*-1} \equiv M_T^{-1}(v^*)$, satisfies $v^{*-1} < v^*$. By continuity of M_T , there is a fixed point of (1.33) with $p = n$ between v^{*-1} and v^* . (The discontinuity of M_T occurs exactly at v^{*-1} where it is right continuous.)

To show that there can be two stable fixed points, we suppose that nT is very close to but greater than T^* . There is a small $\delta > 0$ such that $M_T(v^{*-1} - \delta) < v^{*-1} - \delta$ with $p = n + 1$ in (1.33). Let \hat{v} be the unique value of v for which

$$T = \int_{\hat{v}}^{v^*} \frac{dv}{G_+(v)}.$$

Then $M_T(\hat{v}) > \hat{v}$ with $p = n + 1$. Notice that $\hat{v} < v^{*-1}$ if nT is close to T^* , so that the continuity of M_T guarantees the existence of a fixed point between \hat{v} and $v^{*-1} - \delta$. For this point $p = n + 1$ in (1.33).

It is clear that a fixed point of the mapping is lost as $nT \rightarrow T^*$. Thus, the left endpoint of the n th interval is $t_n = T^*/n$. The right endpoint s_n is that value for which a fixed point \hat{v} of (1.33) with $p = n$ satisfies

$$(1.35) \quad s_n = \int_{v^*}^{\hat{v}} \frac{dv}{G_-(v)}.$$

From the above arguments it follows that $t_n < s_{n+1}$. Of course these endpoints will be changed somewhat because of $O(\varepsilon)$ effects, which we have ignored.

Notice that the wavetrain produced by a fixed point of (1.31) is periodic in time, but not space. After a pulse is produced it must change shape according to (1.28) until a steady spatial structure with period nT is formed. For this asymptotic structure we must have values v_l and v_{tr} in the leading and trailing shock, respectively, which satisfy

$$nT = \int_{v_l}^{v_{tr}} \frac{dv}{G_+(v)} + \int_{v_{tr}}^{v_l} \frac{dv}{G_-(v)}, \quad |c_+(v_l)| = |c_-(v_{tr})|.$$

We can illustrate these results for the Fitzhugh-Nagumo caricature (1.2)'. For these dynamics the number T^* is

$$(1.36) \quad T^* = \ln \left(\frac{1/2 + \alpha}{1/2 - \alpha} \cdot \frac{1 - \alpha}{\alpha} \right),$$

and the mapping (1.33) is given by

$$(1.37) \quad v_{k+1} = \frac{1 - \alpha}{\alpha} (1 - v_k) e^{-pT} \quad \text{provided} \quad v_{k+1} < v^* = \frac{1}{2} - \alpha.$$

For this mapping, the comparison (1.34) always holds since

$$(1.38) \quad \begin{aligned} |\hat{v}_1 - \hat{v}_2| &= \frac{1 - \alpha}{\alpha} |v_2 - v_1| e^{-pT} \\ &\leq \frac{1 - \alpha}{\alpha} |v_2 - v_1| e^{-T^*} = \left(\frac{1/2 - \alpha}{1/2 + \alpha} \right) |v_2 - v_1|, \quad 0 < \alpha < \frac{1}{2}, \end{aligned}$$

so that fixed points are stable. The endpoints of the $1:n$ response regions are $t_n = T^*/n$ and s_n , where

$$(1.39) \quad s_n = \ln \frac{1/2 - \alpha}{\hat{v}},$$

and where \hat{v} is determined by

$$\left(\frac{1/2 - \alpha}{\hat{v}} \right)^n = \left(\frac{1 - \alpha}{\alpha} \right) \left(\frac{1 - \hat{v}}{\hat{v}} \right).$$

Finally, observe that a steady periodic wavetrain with leading shock structure v_1 has trailing shock structure $v_{tr} = 1 - 2\alpha - v_1$ and period

$$T = \ln \left(\frac{1 - v_1}{v_1} \cdot \frac{1 - 2\alpha - v_1}{2\alpha + v_1} \right).$$

Thus, for a given period T the asymptotic structure of the leading shock is

$$v_1 = \frac{(\alpha - 1)e^{-T} - \alpha + (\alpha^2 + (1 - 2\alpha^2)e^{-T} + \alpha^2 e^{-2T})^{1/2}}{1 - e^{-T}},$$

and the speed is given by (1.18).

1.6. Numerical computations. In this section we present the results of some numerical computations performed by J. Rinzel. Equations (1.1) with piecewise linear dynamics (1.2)' were solved with $\alpha = 0.3$ and $\varepsilon = 0.05$ using the standard Crank-Nicolson difference approximation. The equations were solved on $0 \leq x \leq L$ with even symmetry about $x = 0$ and $u_t + \theta u_x = 0$ at $x = L$, where $\theta = 0.7$ is the observed numerical speed of the solitary pulse solution.

Two different types of initial data were specified to compare with the results of this analysis. In the first case, the spatial initial data were taken from the space clamped ($D_1 = D_2 = 0$) dynamics and stretched in space with $x = \theta t$. In Figs. 2A and 2B, the profiles of u and v are given for various values of time t , and in Fig. 2C the phase plane portrait of u and v is shown for these same values of t . The important thing to observe about this solution is that although the pulse is initiated with trailing shock at $v = v_{\max}$, the value of v internal to the trailing shock quickly decreases and the length of the pulse shortens to its stable equilibrium value. The leading edge of the pulse assumes its asymptotic speed very quickly, and the trailing pulse reaches its asymptotic speed somewhat later.

The second set of initial data were chosen to simulate an impulse at a local site. A square superthreshold step was given to u as initial data on $0 \leq x \leq 5$; the system was otherwise at rest. In Figs. 3A, B, and C, the spatial profiles of u and v and the phase plane portrait of u and v are given, respectively, for various values of t .

Again an important observation is that the early shape of the pulse on $0 \leq x \leq 5$ is like that of the space clamped dynamics. As time progresses, the trailing edge speeds up to reach its correct asymptotic position.

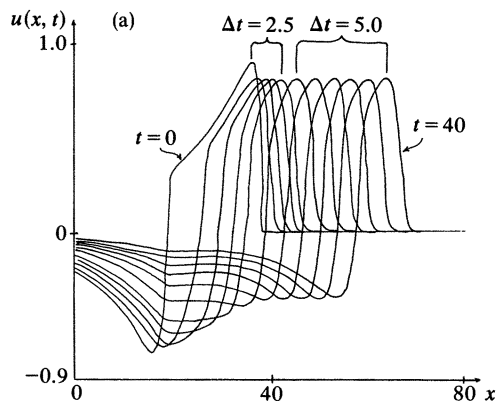


FIG. 2A

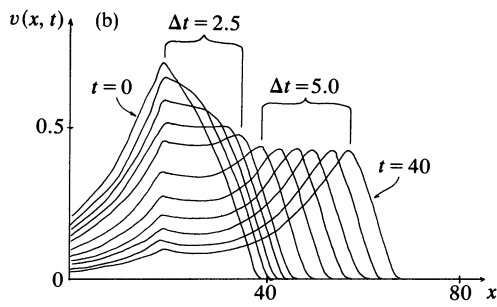


FIG. 2B

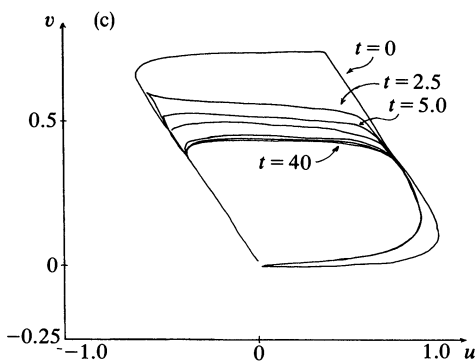


FIG. 2C

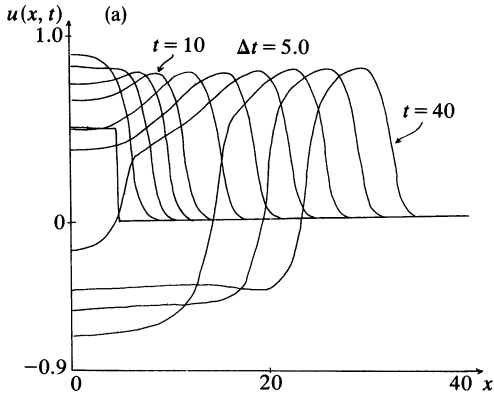


FIG. 3A

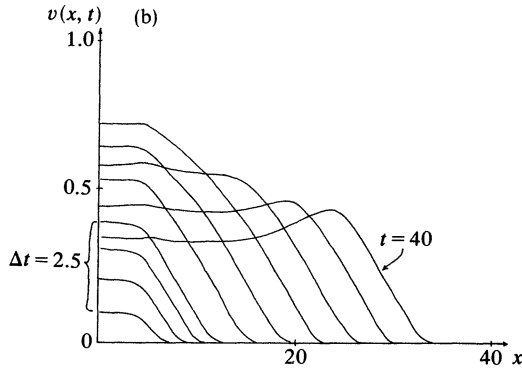


FIG. 3B

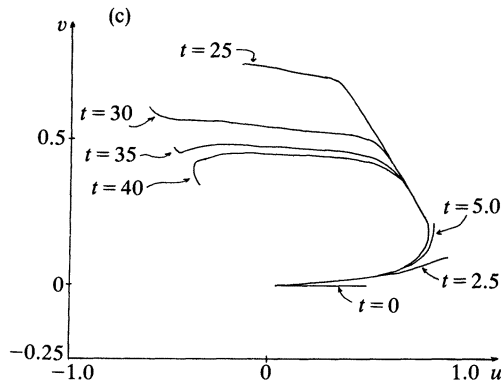


FIG. 3C

1.7. Other dynamics. With different assumptions on the neutral curve $g(u, v) = 0$, it is possible to have different types of dynamics which support different types of wavefront propagation. In this section we apply the inner and outer expansions of the previous sections to discuss briefly the response of these different dynamics to initial data. Similar dynamics have been discussed in [8].

Suppose the general properties of $f(u, v)$ assumed in § 1.1 continue to hold. The different cases we discuss below come from different assumptions on the intersections of $g(u, v) = 0$ with $f(u, v) = 0$. In all cases, intersections on either of the curves $u = u_{\pm}(v)$ are assumed to be stable uniform steady state solutions of (1.1). Thus, $g(u, v)$ is assumed to be negative above and positive below the neutral curve $g(u, v) = 0$. In three of the four cases that follow we assume that $g(u, v) = 0$ has intersections on all three branches of $f(u, v) = 0$. The intersections on $u = u_{\pm}(v)$ are denoted (u_{\pm}, v_{\pm}) , respectively. The third intersection on the branch $u = u_*(v)$ is an unstable steady state solution of the equations and has no effect on the wave motion which results. The value v^* is defined in (1.23).

The main observations about the inner and outer solutions remain unchanged: If a shock has internal structure v , its speed $c_{\pm}(v)$ determines the front and back of the shock. The value of v inside the shock is determined by the outer dynamics ahead of the shock.

Case I. $v_- < v^* < v_+$; there are two stable solitary wave fronts, one with speed $c_{\pm}(v_-)$ which provides a permanent transition from $u_-(v)$ ahead to $u_+(v)$ behind at $v = v_-$, and the second with speed $c_{\pm}(v_+)$ which provides a permanent transition from $u_+(v)$ ahead to $u_-(v)$ behind at $v = v_+$. These two shocks are the only stable single front

solutions which can evolve from initial data. It is interesting to observe that if the initial data satisfy $u_0(x) \rightarrow u_{\pm}, v_0(x) \rightarrow v_{\pm}$ as $x \rightarrow \pm\infty$, with a single crossing of the dividing curve $u = u_*(v)$, then the steady state which eventually dominates is (u_+, v_+) if $v_0(x)$ crosses $u_*(v)$ with $v > v^*$ and is (u_-, v_-) if $v_0(x)$ crosses $u_*(v)$ with $v < v^*$.

In addition to these wave front solutions, there is a stable solitary pulse with leading and trailing edges traveling at speed $\min\{|c_+(v_{\pm})|\}$. This pulse has structure the same as the solitary pulse of §§ 1.2, 1.3. Finally, as in § 1.4, there are stable periodic wavetrains for speeds smaller than $\min\{|c_+(v_{\pm})|\}$, with dispersion relation (1.30).

Case II. $v_{\pm} > v^*$; there is a unique stable wavefront moving with speed $|c_{\pm}(v_+)|$ which provides a transition from $u_+(v)$ ahead to $u_-(v)$ behind at $v = v_+$. There are no stable, steady periodic structures.

Case III. $v_- > v^* > v_+$; the only steady shock has speed zero providing a transition from $u_-(v)$ on one side to $u_+(v)$ on the other at $v = v^*$. Many spatial structures can be built from this stationary shock using the outer solution (smoothed by diffusion) between the shocks at various spatial locations.

Case IV. The curve $g(u, v) = 0$ has no intersection with $u = u_{\pm}(v)$ and a single intersection with $u = u_*(v)$. In this case the dynamics are those of a relaxation oscillation. There are stable periodic wavetrains like those of § 1.4. The relationship between wavelength, period, and speed (the dispersion relation ([16], [18])) is given by (1.30). Notice that these wavetrains do not use all of the dynamics provided by the curve $f(u, v) = 0$. In all but exceptional cases, the shocks occur for $v < v_{\max}$ and $v > v_{\min}$, so that the spatial structure of these wavetrains is not the same as the temporal behavior of the $D_1 = D_2 = 0$ dynamics.

PART II. Waves in two dimensions.

2.1. Equations of the leading edge. In a two-dimensional region, the dynamics of the excitable medium is again governed by (1.1) with $\nabla^2 = \partial^2/\partial x^2 + \partial^2/\partial y^2$. The behavior of the medium is only slightly complicated by the higher dimensionality of the space. The outer equations remain the same; specifically, away from any front

$$(1.11) \quad v_t = G_{\pm}(v), \quad f(u, v) = 0.$$

We also know from previous considerations that as a front moves, its internal structure is determined by the outer dynamics ahead of it. The added complication we face here is to calculate specifically how the shock moves.

To determine how the shock moves we suppose that at time t , there is a shock along the curve in space parameterized by s

$$(2.1) \quad \mathbf{R}(s, t) = X(s, t)\mathbf{i} + Y(s, t)\mathbf{j}.$$

We introduce a local coordinate system with the curve $\mathbf{R}(s, t)$ as one of the axes,

$$(2.2a) \quad xi + yj = \mathbf{R}(s, t) + \eta \mathbf{N}(s, t), \quad t = \tau,$$

where $\mathbf{N}(s, t)$ is the unit normal to $\mathbf{R}(s, t)$

$$(2.2b) \quad \mathbf{N}(s, t) = \frac{Y_s \mathbf{i} - X_s \mathbf{j}}{\sqrt{X_s^2 + Y_s^2}}.$$

Equation (2.2) can be written as

$$(2.3) \quad x = X + \frac{\eta Y_s}{\sqrt{X_s^2 + Y_s^2}}, \quad y = Y - \frac{\eta X_s}{\sqrt{X_s^2 + Y_s^2}}, \quad t = \tau.$$

To carry out the change of coordinate system (2.3), we calculate how derivatives transform. It is straightforward to show that

$$\begin{aligned}
 \frac{\partial}{\partial x} &= \frac{X_s}{X_s^2 + Y_s^2} \frac{1}{1 + \eta K} \frac{\partial}{\partial s} + \frac{Y_s}{(X_s^2 + Y_s^2)^{1/2}} \frac{\partial}{\partial \eta}, \\
 (2.4a) \quad \frac{\partial}{\partial y} &= \frac{Y_s}{X_s^2 + Y_s^2} \frac{1}{1 + \eta K} \frac{\partial}{\partial s} - \frac{X_s}{(X_s^2 + Y_s^2)^{1/2}} \frac{\partial}{\partial \eta}, \\
 \frac{\partial}{\partial t} &= \frac{-1}{1 + \eta K} \frac{1}{X_s^2 + Y_s^2} \left[X_s X_\tau + Y_s Y_\tau + \eta \frac{X_s X_{s\tau} - Y_s X_{s\tau}}{(X_s^2 + Y_s^2)^{1/2}} \right] \frac{\partial}{\partial s} - c(s, \tau) \frac{\partial}{\partial \eta} + \frac{\partial}{\partial \tau},
 \end{aligned}$$

where

$$(2.4b) \quad K(s, \tau) = \frac{X_s Y_{ss} - Y_s X_{ss}}{(X_s^2 + Y_s^2)^{3/2}}$$

is the curvature, and

$$(2.4c) \quad c(s, \tau) = \frac{X_\tau Y_s - Y_\tau X_s}{(X_s^2 + Y_s^2)^{1/2}}$$

is the speed of propagation of $\mathbf{R}(s, \tau)$ normal to itself. In fact

$$(2.5a) \quad \mathbf{R}_\tau = c\mathbf{N} + \alpha\mathbf{T},$$

where \mathbf{N} and \mathbf{T} are the unit normal and tangent vectors respectively, and

$$(2.5b) \quad \alpha = \frac{X_s X_\tau + Y_s Y_\tau}{(X_s^2 + Y_s^2)^{1/2}}.$$

Using (2.4), we find that in the new variables the Laplacian becomes

$$(2.6) \quad \nabla^2 u = \left(\frac{1}{1 + \eta K} \right)^2 \frac{\partial^2 u}{\partial s^2} + \frac{1}{2} \frac{\partial}{\partial s} \left(\frac{1}{1 + \eta K} \right)^2 \frac{\partial u}{\partial s} + \frac{\partial^2 u}{\partial \eta^2} + \frac{K}{1 + \eta K} \frac{\partial u}{\partial \eta}.$$

We are now ready to find the inner equations. We set $\eta = \varepsilon \xi$ in (2.4) and (2.6) applied to (1.1), and then set $\varepsilon = 0$. The resulting inner equations are

$$\begin{aligned}
 (2.7) \quad & \frac{\partial^2 u}{\partial \xi^2} + c(s, \tau) \frac{\partial u}{\partial \xi} + f(u, v) = 0, \\
 & c(s, \tau) \frac{\partial v}{\partial \xi} = 0.
 \end{aligned}$$

The inner equations (2.7) are not surprising. They imply that the value of v internal to the shock is independent of ξ , and that the speed of the shock is again determined by the eigenvalue problem (1.16).

Although (2.7) are the lowest order equations for the inner expansion, the coordinate system (2.3) is not the correct coordinate system to find higher order corrections to (2.7). The singularities of (2.6) at $\eta = -1/K$ are an artifact of the coordinate system that prevent η from becoming large.

One way to find a singularity-free coordinate system is to solve Laplace's equation $\nabla^2 \eta = 0$ for the coordinate η on an infinite strip which contains the arc $\mathbf{R}(s, t)$ in its interior. Require $\eta = \pm 1$ (say) on the two boundaries, and $\eta = 0$ on $\mathbf{R}(s, t)$. Although this problem is overdetermined, the solution is well-defined and smooth on each of the two interior regions separated by $\mathbf{R}(s, t)$. The solution on the entire strip is continuous

and has a discontinuous derivative on the curve $\mathbf{R}(s, t)$ but is smooth elsewhere. The conjugate function to η defines the orthogonal trajectories which are the level curves for s . This completes the description of a singularity-free coordinate system.

The system (2.3) is the first-order approximation to such a singularity-free system, and (2.7) is valid whenever the radius of curvature of $\mathbf{R}(s, t)$ is large compared with ε . Higher order corrections to the inner equations (2.7) require higher order approximations to the singularity-free system.

In summary, away from shocks the solution evolves according to (1.11). Shocks, either leading or trailing, move with normal velocity determined by the internal value of v and (1.16). The internal value of v is determined by the outer dynamics ahead of the shock.

2.2. Self-sustained wave motion. In an unbounded simply connected two-dimensional region, the solutions that we find have little more interest than those in a one-dimensional domain. There are no self-sustained oscillations unless special geometric properties hold. In particular, if the medium has one or more “dead” regions, that is, bounded regions with impermeable boundaries inside of which the equations (1.1) do not apply, then self-sustained wave motion can exist. In this section we describe some of the self-sustained motion which can occur in multiply connected regions.

By choosing to examine multiply connected regions with dead spaces, we have avoided a difficult mathematical question. In [26] it was stated that without such dead spaces self-sustained wave motion cannot occur. Furthermore, experiments seem to require a large dead region ([25]). On the other hand, numerical calculations ([6], [29]) have managed to produce spiral motion without the benefit of a dead space. Previous mathematical results on geometrical patterns with centers ([12], [18]) are also invalid near the center of the pattern.

Waves on a ring. Perhaps the easiest way to produce self-sustained motion in an excitable medium is on a ring of radius R_0 . To initiate the pulse we assume that the initial data create a single leading edge with $v < v^*$ and a single trailing edge with $v > v^*$. To set up this type of initial data requires some experimental dexterity (see [25] and [26] for a discussion of the initiation of self-sustained wave motion).

Suppose we know the internal structure $v_1(t)$ of the leading shock. Then the trailing shock is determined by (1.25). Since we are on a ring, the internal structure $v_1(t)$ is determined by that of the trailing shock through (1.28). Since the ring has circumference $2\pi R_0$, the sum of the two separations must be $2\pi R_0$. Thus, the values v_1 and v_2 and separations s_1 and s_2 of the leading and trailing shocks are determined by

$$(2.8a) \quad \frac{ds_1}{dt} = c_-(v_1) - c_+(v_2),$$

$$s_1 = \int_{t-\tau}^t c_-(v_1(\eta)) d\eta, \quad \tau = \int_{v_1(t-\tau)}^{v_2} \frac{dv}{G_+(v)},$$

and

$$(2.8b) \quad \frac{ds_2}{dt} = c_+(v_2) - c_-(v_1),$$

$$s_2 = \int_{t-\sigma}^t c_+(v_2(\eta)) d\eta, \quad \sigma = \int_{v_2(t-\sigma)}^{v_1} \frac{dv}{G_-(v)},$$

$$(2.8c) \quad s_1 + s_2 = 2\pi R_0,$$

with initial data specified over the entire ring.

The most important observation about this system of equations is that there is a unique steady-state solution. If we choose v_1 and v_2 such that $c_-(v_1) = c_+(v_2)$, and such that

$$(2.9a) \quad 2\pi R_0 = c_-(v_1) \int_{v_1}^{v_2} \left(\frac{dv}{G_+(v)} - \frac{dv}{G_-(v)} \right),$$

then (2.8) is satisfied with steady separations

$$(2.9b) \quad s_1 = c_-(v_1) \int_{v_1}^{v_2} \frac{dv}{G_+(v)}, \quad s_2 = c_-(v_1) \int_{v_2}^{v_1} \frac{dv}{G_-(v)}.$$

The period T of this periodic motion is

$$(2.9c) \quad T = \frac{2R_0}{c_-(v_1)} \equiv \int_{v_1}^{v_2} \left(\frac{1}{G_+(v)} - \frac{1}{G_-(v)} \right) dv.$$

The qualitative relationship between R_0 , c , and T for these periodic motions is easy to deduce. We assumed earlier that $c_-(v)$ is a monotonic decreasing function of v , $c_-(v^*) = 0$. The value v_2 for which $c_+(v_2) = c_-(v_1)$ is a monotonic decreasing function of v_1 , so that T is a monotonic decreasing function of v_1 . Since $2\pi R_0 = T(v_1) \cdot c_-(v_1)$, the wavelength $2\pi R_0$ is also a monotonic decreasing function of v_1 . Eliminating the intermediate variable v_1 , we see that both the speed c and period T are monotonic increasing functions of R_0 , the radius of the ring.

Spirals. Suppose that the medium contains a circular dead space at its center, and the boundary of this region is a ring of radius r_0 . We would like to solve the evolution equations (1.11), (2.5), and (1.16) on the exterior of this circular region with arbitrary initial data. Although it is not difficult to understand the evolution of these fronts in general, it is very difficult to handle this problem explicitly. Short of this ideal situation we will show that steady solutions of this problem are spirals.

The solution of this initial value problem requires that we specify two more pieces of information: the initial data and boundary conditions. The initial data must be such that on one arc which meets the boundary a leading shock is initiated with $v < v^*$ and on a second arc, a trailing shock is initiated with $v > v^*$. As before, setting up initial data (or experimental conditions) which produce spiral patterns is a nontrivial problem ([25], [26]). To specify boundary data we observe that since a shock propagates with local normal velocity $c(v)$, then the shock locus $\mathbf{R}(s, \tau)$ must meet the boundary at an angle of less than or equal to $\pi/2$, where the angle is measured between the front of the shock and the boundary. In fact a shock impinging upon a boundary does so at an angle less than $\pi/2$, but if the boundary is curving away from the region ahead of the shock, then the shock must meet the boundary at angle $\pi/2$.

The basic idea of [26] was that shocks move with constant velocity normal to themselves. This intriguing idea is not entirely correct in light of the analysis of § 2.1. It is still possible that there are steady solutions which have constant normal velocity. If this is the case, then the perpendicular distance between any two shocks must be independent of position in space, so that the outer solution produces the same constant speed (through (1.16)) everywhere.

Suppose (2.5) has speed c constant independent of s and τ . One can easily verify that one solution of these equations in polar coordinates is

$$(2.10) \quad \tan \psi - \psi = \theta + \frac{ct}{r_0}, \quad r = r_0 \sec \psi.$$

For consistency with the outer solution (1.11) we must pick c to be the speed of the steady shock on a ring of radius r_0 given by (2.9). With this speed c , we observe that the solution (2.10) meets the circle of radius r_0 at an angle $\pi/2$, and is indeed a spiral. Furthermore, any straight line segment which is tangent to the circle and extends to infinity in the direction of forward motion of the spiral intersects the locus (2.10) orthogonally. The distance d between any two intersections is always $d = 2\pi r_0 \equiv cT$. Clearly, this distance is the perpendicular distance between points on the spiral arc (2.10) which is a constant independent of space or time.

It is possible to extend this observation to more general central regions.

PROPOSITION 4. *Suppose R_0 is a bounded dead region whose convex hull has perimeter D_0 . Let c and T be the speed and period of a steady periodic pulse with wavelength D_0 . Then the spatial configuration of the steady self-sustaining wavefront is the involute of the convex hull of R_0 , which moves with normal speed c and has temporal period T and wavelength D_0 .*

The involute of a convex region is the locus of a point on a string which is unwrapped from around the region. To see that the perpendicular distance between arc segments is always the same, mark two points on the string at a distance D_0 apart. Observe that both points trace the same locus, and are separated by distance D_0 , which is the perpendicular distance between arcs.

Interference patterns. If there are two (or more) regions, say R_1 and R_2 , in the domain which generate spirals, then when the spiral patterns meet, the possibility exists that interesting interference patterns result. Recall that when two leading shocks meet, they annihilate each other. When two curved arcs meet they first collide at a point of tangency, and as they continue to move forward, sharp corners are produced at the intersection. In such a region the analysis of § 2.1 breaks down. However, there are still some facts that can be gleaned.

Suppose that $D_1(R_1) < D_2(R_2)$, where $D_i(R_i)$ is the perimeter of the convex hull of R_i , $i = 1, 2$. The steady patterns generated by R_1 and R_2 are involutes of the respective convex hulls. The generators of these involutes are the family of line segments which are tangent to the boundary and extend to infinity in the direction of forward motion of the shock arc. Recall that the perpendicular distance between arcs is measured along a generator. There is exactly one line segment which is a generator for both curves. Since the involutes intersect their generators at right angles, the arcs from R_1 and R_2 meet somewhere along their common generator.

Suppose the arcs from R_1 and R_2 meet at some time t at some point along the common generator. Then at time T_1 later, an arc from R_1 again occupies the point of first intersection. Since $T_1 < T_2$, the arc from R_2 has not yet reached this point. Therefore we observe that

RULE 1. *If $D_1 < D_2$, the point at which arcs from R_1 and R_2 intersect moves toward R_2 along the unique common generator.*

In addition to this point where arcs meet initially, there is an arc through this point which separates the region of influence of R_1 from that of R_2 . It is also apparent that this arc of demarcation moves steadily toward R_2 . As soon as this line touches the boundary of R_2 , the spirals from R_2 are terminated and the space is soon filled with arcs that are generated by R_1 .

We can deduce some qualitative information about the shape of the dividing arc. Near any point where two arcs form a corner, the pattern resembles the intersection of two families of parallel lines, with wavelength D_1 and D_2 . The lines through the points of intersection makes an angle θ_i with the set of parallel lines with wavelength D_i . Then

$$\frac{D_1}{\sin \theta_1} = \frac{D_2}{\sin \theta_2},$$

so that $\theta_1 < \theta_2$. From this we observe that

RULE 2. *If $D_1 < D_2$, then the arc separating the regions of influence of R_1 and R_2 is concave toward R_1 .*

This analysis of interference patterns has two deficiencies. First, as mentioned before, the analysis breaks down when arcs intersect because the intersection introduces a corner. Second, in the neighborhood of the line of demarcation, the assumption of steady arc propagation is not correct. Nevertheless, although detailed calculations based on the steady assumption are not correct, qualitative features of interference patterns appear to be correct.

Finally, we observe that if two similar central regions with $D_1 = D_2$ are close together, the spiral patterns from the two merge along a line between the two, and at large distances from the center appear to be concentric rings. These interference patterns are called pacemakers. It is apparent that different sized cores will produce pacemakers of different frequencies.

Acknowledgment. I am indebted to Dr. John Rinzel of the National Institute of Health for his valuable discussion and numerical computations.

REFERENCES

- [1] D. G. ARONSON AND H. F. WEINBERGER, *Nonlinear diffusion in population genetics, combustion and nerve propagation*, in Proceedings of the Tulane Program in Partial Differential Equations and Related Topics, Lecture Notes in Mathematics, 446, Springer, New York, 1975.
- [2] N. F. BRITTON AND J. D. MURRAY, *Threshold, wave and cell-cell avalanche behavior in a class of substrate inhibition oscillators*, J. Theor. Biol. 75 (1979).
- [3] G. A. CARPENTER, *Traveling wave solutions of nerve impulse equations*, Doctoral thesis, University of Wisconsin, Madison, WI, 1974.
- [4] R. CASTEN, H. COHEN AND P. LAGERSTROM, *Perturbation analysis of an approximation to Hodgkin-Huxley Theory*, Quart. Appl. Math., 32 (1975), pp. 365–402.
- [5] D. S. COHEN, J. C. NEU AND R. R. ROSALES, *Rotating spiral wave solutions of reaction-diffusion equations*, this Journal, 35 (1978), pp. 536–547.
- [6] TH. ERNEUX AND M. HERSCKOWITZ-KAUFMAN, *Rotating waves as asymptotic solutions of a model chemical reaction*, J. Chem. Phys., 66 (1977), pp. 248–250.
- [7] B. C. FARLEY, *Some results of computer simulation of neuron-like nets*, Fed. Proc. 21 (1962), pp. 92–
- [8] P. C. FIFE, *Singular perturbation and wave front techniques in reaction-diffusion problems*, Proc. AMS-SIAM Symposium on Asymptotic Methods and Singular Perturbations, New York, 1976.
- [9] ———, *Mathematical Aspects of Reacting and Diffusing Systems*, Lecture Notes in Biomathematics, Vol. 28, Springer-Verlag, New York, 1979.
- [10] P. C. FIFE AND J. B. MCLEOD, *The approach of solutions of nonlinear diffusion equations to traveling front solutions*, Arch. Rat. Mech. Anal., 65 (1977), pp. 335–361.
- [11] M. GARDNER, *Mathematical games*, Sci. Amer., Oct. 1970, pg. 120, Feb. 1971, pg. 112.
- [12] J. M. GREENBERG, *Periodic solutions to reaction-diffusion systems*, this Journal, 30 (1976), pp. 199–205.
- [13] J. M. GREENBERG AND S. P. HASTINGS, *Spatial patterns for discrete models of diffusion in excitable media*, this Journal, 34 (1978), pp. 515–523.
- [14] S. P. HASTINGS, *On the existence of homoclinic and periodic orbits for the Fitzhugh-Nagumo equations*, Quart. J. Math. Oxford Ser. 2, 27 (1976), pp. 123–134.

- [15] A. L. HODGKIN AND A. F. HUXLEY, *A quantitative description of membrane current and its application to conduction and excitation in nerve*, J. Physiol., 117 (1952), pp. 500–544.
- [16] L. N. HOWARD AND N. KOPELL, *Wave trains, shock fronts, and transition layers in reaction-diffusion equations*, in Mathematical Aspects of Chemical and Biochemical Problems and Quantum Chemistry, D. S. Cohen, ed., SIAM-AMS Proceedings, Vol. 8, American Mathematical Society, Providence RI, 1974.
- [17] H. R. KARFUNKEL AND F. F. SEELIG, *Excitable chemical reaction systems, I. Definition of excitability and simulation of model systems*, J. Math. Biol., 2 (1975), pp. 123–132.
- [18] N. KOPELL AND L. N. HOWARD, *Plane wave solutions to reaction-diffusion equations*, Stud. Appl. Math., 52 (1973), pp. 291–328.
- [19] V. I. KRINSKI, *Excitation wave propagation during fibrillation*, in Biological and Biochemical Oscillations, B. Chance, E. K. Pye, A. K. Ghosh, B. Hess, eds., Academic Press, New York, 1973, pp. 329–341.
- [20] H. P. MCKEAN, *Nagumo's equation*, Adv. in Math., 4 (1975), pp. 209–223.
- [21] C. K. MOE, W. C. RHEINOLDT AND J. A. ABILDOKOV, *A computer model of atrial fibrillation*, Am. Heart. J., 67 (1964), pp. 200–220.
- [22] P. ORTOLEVA AND J. ROSS, *Theory of propagation of discontinuities in kinetic systems with multiple time scales: fronts, front multiplicity and pulses*, J. Chem. Phys. 63 (1975), pp. 3398–3408.
- [23] C. S. PESKIN, *Partial Differential Equations in Biology*, Courant Institute of Mathematical Sciences (Lecture Notes), New York University, 1976.
- [24] J. RINZEL AND J. B. KELLER, *Traveling wave solutions of a nerve conduction equation*, Biophys. J., 13 (1973), pp. 1313–1337.
- [25] M. SHIBATA AND J. BURES, *Optimum topographical conditions for reverberating cortical spreading depression in rats*, J. Neurobiology, 5 (1974), pp. 107–118.
- [26] N. WEINER AND A. ROSENBLUETH, *The mathematical formulation of the problem of conduction of impulses in a network of connected excitable elements, specifically in cardiac muscle*, Arch. Inst. Cardiologia de Mexico, 16 (1946), pp. 205–265.
- [27] A. T. WINFREE, *Spiral waves of chemical activity*, Sci., 175 (1972), pp. 634–636.
- [28] ———, *Rotating chemical reactions*, Sci. Amer., 230 (6) (1974), pp. 82–95.
- [29] ———, *Rotating solutions to reaction-diffusion equations in simply connected media*, in Mathematical Aspects of Chemical and Biochemical Problems and Quantum Chemistry, D. S. Cohen, ed., SIAM-AMS Proceedings, Vol. 8, American Mathematical Society, Providence RI, 1974.